Bull. Chem. Soc. Jpn., 58, 2756—2762 (1985) [Vol. 58, No. 10

Electronic Structure and Lattice Distortion of Benzene Anion

Minoru Kimura,[†] Hiroyuki Kawabe, Kiyoshi Nishikawa, and Shigeyuki Aono[*]
[†]*Department of Physics, Faculty of Science, Kanazawa University, Marunouchi, Kanazawa 920*
Department of Chemistry, Faculty of Science, Kanazawa University, Marunouchi, Kanazawa 920

(Received April 27, 1985)

Electronic structure, especially the charge density or the spin density of the benzene anion (exactly dihydrophenylide ion) is investigated by the Hubbard Hamiltonian with vibronic interaction. Two limiting cases, *i.e.*, $I/\beta \ll 1$ and $I/\beta \gg 1$ (I is the electron repulsion on site, β the absolute value of transfer integral.) are analytically examined. For whole range of this ratio, the numerical calculation has been performed. The actual system falls into the latter case, where the electron correlation produces a strong effect on the spin density distribution.

The benzene molecule is a typical subject for theories of electronic states of molecules, while the benzene anion is of interest also from physical viewpoints. In the molecular orbital theory, the benzene molecule has the unoccupied doubly degenerate orbitals. The odd electron of the benzene anion, therefore, would equally populate on these degenerate levels.

If the vibronic coupling exists, the degenerate levels are strongly coupled through an interaction with a certain mode of the vibration, and then the degeneracy is removed to lead to a distorted ground state, *i.e.*, the so-called Jahn-Teller effect arises. Almost all the studies have been made along the above-mentioned simple picture.[1–6] Even in the elaborated work,[4] the electronic state was considered within a single-particle picture for the odd electron, which neglects the role of electron repulsion.

Recently similar problems have been studied in solid state physics, *e.g.*, the study of various ordered phases in the infinite chain molecule.[7] In this decade the so-called many-body technique employed in these investigations are getting familiar also in quantum chemistry. One of the great advantages of the many-body thoery lies in making the investigating procedure systematic and pictorial. In the present work, we employ this method to study the distorted nonuniform ground state in the benzene anion, taking into account the most dominant part of the electron interaction.

Model Hamiltonian and One-electron Theory

Let us consider the system to be described by the P.P.P. Hamiltonian with terms which is responsible for lattice distortion,

$$H = \sum_{r,\sigma}\alpha_r n_{r\sigma} - \sum_{r,\sigma}(\beta_{r,r+1}a^{+}_{r\sigma}a_{r+1\sigma}+\text{h.c.}) + \frac{1}{2}\sum_{r,s,\sigma}I_{r,s}n_{r\sigma}n_{s-\sigma} + \frac{1}{2}M\Omega^2\sum_{r}Q_r^2, \tag{1}$$

where α_r is the Coulomb integral of the site r, $\beta_{r,s}$ is the resonance integral and $I_{r,s}$ the electron–electron interaction constant. The last term of Eq. 1 represents the elastic energy due to the distortion Q_r of the site r from its C_6-symmetric configuration. It includes the compressional energy of σ electrons. In the undistorted symmetric configuration, α_r and $\beta_{r,s}$ are uniform. Therefore, so long as Q_r is small, they are expanded in Q_r and can be written as

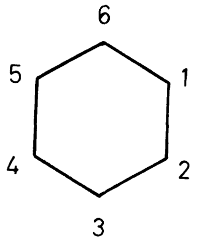

Fig. 1. Site numbers for the benzene anion.

$$\alpha_r = \alpha_0 + gQ_r + \frac{1}{2}\Delta\alpha(\delta_{r,3}+\delta_{r,6}), \tag{2}$$

$$\beta_{r,r\pm1} = \beta + g'Q_r, \tag{3}$$

where g and g' are the expansion coefficients. The last term of Eq. 2 represents the perturbation arising from the interaction with solvent which may be added, say, at the sites r=3 and 6 (Fig. 1), which reduces the molecular symmetry from C_6 to C_2. It will be time-dependent in view of thermal motion of solvent molecules. However, if we assume that it is sufficiently slow as compared to motion of the phase of the distortion, we can consider it as a static perturbation. As will be shown below, its effect is to pin up the phase of the distortion at the particular site so as to minimize the total energy.

Equation 3 has been used to study the bond-alternation in polyene (for example the model of Su, Schriefer and Heeger in considering polyacetylene[7]), while Eq. 2 was considered by Holstein[8] to study the polaron in molecular chains. The second terms of Eqs. 2 and 3 both contribute to the change of the energy of the electrons due to the distortion. However, in the present study, they yield essentially the same physical effect except for the difference of the phases of distortion, so that we shall take only the change of α_r of Eq. 2 into account, and consider

$$\beta_{r,r\pm1} = \beta \tag{4}$$

as a constant.

The electron–electron interaction plays an important role in the electron distribution, which was not considered in the early works.[1–7] However, the full consideration of electron interaction in Eq. 1 is so complex as to preclude physical pictures, therefore we shall consider only the on-site repulsion $I_{r,r}=I$ in order to examine the essential features qualitatively.[9–11]

Then, the Hamiltonian to be considered becomes

$$H = H_0 + H_{\mathrm{int}} + H_{\mathrm{L}}, \tag{5}$$

$$H_0 = -\beta\sum_{r,\sigma}(a^+_{r\sigma}a_{r+1\sigma} + \mathrm{h.c.}), \tag{6}$$

$$H_{\mathrm{int}} = g\sum_{r,\sigma}Q_r n_{r\sigma} + \frac{1}{2}I\sum_{r,\sigma}n_{r\sigma}n_{r-\sigma} + \frac{1}{2}\Delta\alpha\sum_{r,\sigma}n_{r\sigma}(\delta_{r,3}+\delta_{r,6}), \tag{7}$$

$$H_{\mathrm{L}} = \frac{1}{2}M\Omega^2\sum_r Q_r^2. \tag{8}$$

Now, let us outline the one-electron theory of Jahn-Teller distortion. The molecular orbitals given by H_0 have LCAO coefficients at the atomic site r as given by,

$$C_{r,k_n} = 1/\sqrt{6}\,\mathrm{e}^{ik_n r}, \tag{9}$$

where the periodic boundary condition for k_n imposes that

$$k_n = \frac{\pi}{3}n \quad (n=0,\ \pm1,\ \pm2,\ 3), \tag{10}$$

and the one-electron spectrum is given by

$$\varepsilon_n = -2\beta\cos k_n. \tag{11}$$

In the neutral benzene, the orbitals $n=0$ and ±1 are occupied. The odd electron in the benzene anion may occupy either one of the orbitals with $n=+2$ or -2, so that the state of the anion is doubly degenerate (the spin of the odd electron is fixed). Therefore, any perturbation which has the component of C_2-symmetry will remove this degeneracy, even if it may be considerably small. Indeed, if the electron-electron interaction is neglected for a time, the first order perturbation theory gives the splitting of ε_2 as

$$\tilde{\varepsilon}_\pm = \varepsilon_2 \pm \Delta. \tag{12}$$

We express the distortion of C_2-mode, which couples with the orbitals $n=\pm2$, as

$$Q_r = \frac{1}{6}Q(\mathrm{e}^{ik_2 r+i\varphi} + \mathrm{e}^{-ik_2 r-i\varphi}), \tag{13}$$

where Q and φ are the amplitude and the phase of distortion, respectively. Then, Δ is given by

$$\Delta = \frac{1}{6}\{(\Delta\alpha)^2 - gQ\Delta\alpha\cos\varphi + g^2Q^2\}^{1/2}. \tag{14}$$

The odd electron must occupy the level $\tilde{\varepsilon}_-$, so that the energy change caused by the distortion is

$$W = -\Delta + \frac{1}{6}M\Omega^2Q^2. \tag{15}$$

Equation 15 plays the role of adiabatic potential for the system. The ground state configuration is obtained by minimizing W with respect to Q and φ, and as optimum values we obtain

$$\varphi_0 = 0 \text{ or } \pi, \tag{16}$$

according to $\Delta\alpha<0$ or >0, respectively, and

$$Q_0 = g/(2M\Omega^2). \tag{17}$$

The minimum of W is negative, so that the Jahn-Teller distortion is stabilized. The odd electron distribution becomes nonuniform as given by

$$\Delta n_r = \frac{1}{6}(1\mp\cos\frac{2\pi}{3}r), \tag{18}$$

where the sign $\mp$ corresponds to $\Delta\alpha\gtrless0$. Within this approach the spin density distribution is the same as Eq. 18 apart from the factor 1/2 (Fig. 2). Equation 18 is the same as obtained by Hobey and McLachlan.[3]

Green's Function Theory

In benzene the electron repulsion is not considered to be small and the one-electron theory considering only the degenerate orbitals with $n=\pm2$ is too simple to explain the real system. We must consider all the seven electrons together in the framework of the many-body theory, even within the Hartree-Fock scheme. For this purpose it is convenient to introduce the Green's function defined by

$$G^\sigma_{r,s}(t) = -i\langle T[a_{r\sigma}(t)a^+_{s\sigma}(0)]\rangle. \tag{19}$$

Transforming the atomic orbitals into the molecular orbitals, Eq. 19 becomes

$$G^\sigma_{r,s}(t) = \frac{1}{6}\sum_{p,q}G^\sigma_{p,q}(t)\mathrm{e}^{ipr-iqs}, \tag{20}$$

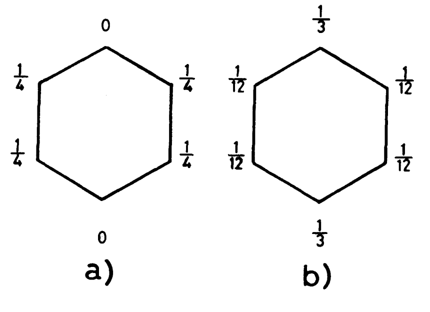

Fig. 2. The electron density distribution in the one-electron theory. a) $\Delta\alpha>0$, b) $\Delta\alpha<0$.

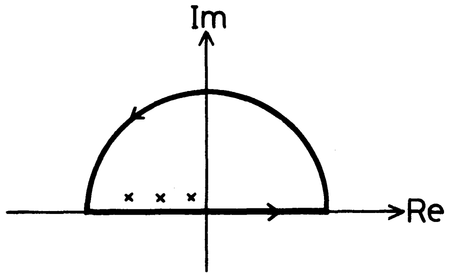

Fig. 3. Closed contour for Eq. 25. The crosses represent the singular points of the Green's function. The contour of integration in the complex plane is the real axis from $-\infty$ to ∞ and the semicircle of the upper half plane.

where

$$G^{\sigma}_{p.q}(t) = -i\langle T[a_{p\sigma}(t)a^{+}_{q\sigma}(0)]\rangle. \tag{21}$$

The Fourier transform of the Green's function is defined as

$$G^{\sigma}_{p.q}(t) = \int_{-\infty}^{\infty}\frac{\mathrm{d}\varepsilon}{2\pi}G^{\sigma}_{p.q}(\varepsilon)\mathrm{e}^{-i\varepsilon t}. \tag{22}$$

It can be expected that the special role played by the C_2-mode of distortion remains important so long as the electron repulsion is not too strong and we thus consider that the dominant components of the Green's function $G^{\sigma}_{p,q}(t)$ are those for $q=p$, $p\pm k$, where we denote as $k\equiv k_2=2\pi/3$, and the other components can be neglected. The electron distribution is then

$$n_{r\sigma} = n_{\sigma} + \sum_{p}(\langle a^{+}_{p+k\sigma}a_{p\sigma}\rangle \mathrm{e}^{-ikr}+\text{c.c.}). \tag{23}$$

The first term of Eq. 23 is the uniform part of the density of the electron

$$n_{\sigma} = \frac{1}{N}\sum_{p}\langle a^{+}_{p\sigma}a_{p\sigma}\rangle = \begin{cases} 4/6 \text{ for spin up} \\ 3/6 \text{ for spin down.}\end{cases} \tag{24}$$

The second term of Eq. 23 represents the non-uniform distribution. It is expressed by the Green's function as

$$\begin{aligned}\langle a^{+}_{p+k\sigma}a_{p\sigma}\rangle &= \frac{1}{i}\lim_{t\to 0^-} G^{\sigma}_{p.p+k}(t) \\ &= \int_{-\infty}^{\infty}\frac{\mathrm{d}\varepsilon}{2\pi i}G^{\sigma}_{p.p+k}(\varepsilon)\mathrm{e}^{-i\varepsilon 0^+}.\end{aligned} \tag{25}$$

The ε-integral of Eq. 25 is estimated by closing the contour on the upper half plane as in Fig. 3 to be

$$\langle a^{+}_{p+k\sigma}a_{p\sigma}\rangle = \sum_{i\in\text{occ}} \text{residue of } G^{\sigma}_{p.p+k}(\varepsilon_i), \tag{26}$$

where ε_i is the i-th pole of the Green's function. The total energy can be expressed also by the Green's function as (see Appendix for details)

$$\begin{aligned}E = \frac{1}{2}\sum_{p.\sigma}\int\frac{\mathrm{d}\varepsilon}{2\pi i}[&(\varepsilon+n_{-\sigma}I+\varepsilon_p)G^{\sigma}_{p.p}(\varepsilon) \\ &+\frac{1}{6}(gQ\mathrm{e}^{i\varphi}+\Delta\alpha)G^{\sigma}_{p.p+k}(\varepsilon) \\ &+\frac{1}{6}(gQ\mathrm{e}^{-i\varphi}+\Delta\alpha)G^{\sigma}_{p.p-k}(\varepsilon)].\end{aligned} \tag{27}$$

Equation 27 can be estimated by the sum of the residue of the occupied levels as expressed by Eq. 26.

Now, the equation of motion for the Green's function leads to[12)]

$$\begin{aligned}i\frac{\partial}{\partial t}G^{\sigma}_{r,s}(t) = \delta_{r,s}\delta(t) &\\ &+\{gQ_r+\frac{1}{2}\Delta\alpha(\delta_{r,3}+\delta_{r,6})\}G^{\sigma}_{r,s}(t) \\ &-\beta\{G^{\sigma}_{r+1,s}(t)-G^{\sigma}_{r-1,s}(t)\} \\ &+I\Gamma^{\sigma}_{r,s}(t),\end{aligned} \tag{28}$$

where

$$\Gamma^{\sigma}_{r,s}(t) = -i\langle T[n_{r-\sigma}(t)a_{r\sigma}(t)a^{+}_{s\sigma}(0)]\rangle \tag{29}$$

is the higher order Green's function. Within the Hartree-Fock scheme $\Gamma^{\sigma}_{r,s}$ is approximated by decoupling as

$$\Gamma^{\sigma}_{r,s}(t) = n_{r-\sigma}G^{\sigma}_{r,s}(t). \tag{30}$$

Then, in the molecular orbital representation the equation becomes

$$\begin{aligned}(\varepsilon-\varepsilon_p-In_{-\sigma})G^{\sigma}_{p,q}(\varepsilon) &- C_{\sigma}G^{\sigma}_{p+k,q}(\varepsilon) \\ &- C^{*}_{\sigma}G^{\sigma}_{p-k,q}(\varepsilon) = \delta_{p,q},\end{aligned} \tag{31}$$

where

$$C_{\sigma} = \frac{1}{6}(gQ\mathrm{e}^{-i\varphi}+\Delta\alpha+D_{-\sigma}), \tag{32}$$

and

$$D_{\sigma} = I\sum_{p}\langle a^{+}_{p+k\sigma}a_{p\sigma}\rangle \tag{33}$$

is determined by Eq. 25. It is easily shown that the total energy is minimized when C_σ and D_σ are real and $\varphi=0$ or π. The system as expressed by Eq. 31 is separated into two sets of equations as illustrated in Fig. 4. Then, the equations for $G_{p,p}$ and $G_{p,p\pm k}$ are expressed as

$$\begin{bmatrix} \varepsilon-\omega_{2,\sigma} & -C_\sigma & -C_\sigma \\ -C_\sigma & \varepsilon-\omega_{0,\sigma} & -C_\sigma \\ -C_\sigma & -C_\sigma & \varepsilon-\omega_{2,\sigma}\end{bmatrix}\begin{bmatrix} G^{\sigma}_{2,q} \\ G^{\sigma}_{0,q} \\ G^{\sigma}_{-2,q}\end{bmatrix} = \begin{bmatrix}\delta_{2,q} \\ \delta_{0,q} \\ \delta_{-2,q}\end{bmatrix}, \tag{34}$$

$$\begin{bmatrix} \varepsilon-\omega_{1,\sigma} & -C_\sigma & -C_\sigma \\ -C_\sigma & \varepsilon-\omega_{3,\sigma} & -C_\sigma \\ -C_\sigma & -C_\sigma & \varepsilon-\omega_{1,\sigma}\end{bmatrix}\begin{bmatrix} G^{\sigma}_{1,q} \\ G^{\sigma}_{3,q} \\ G^{\sigma}_{-1,q}\end{bmatrix} = \begin{bmatrix}\delta_{1,q} \\ \delta_{3,q} \\ \delta_{-1,q}\end{bmatrix}, \tag{35}$$

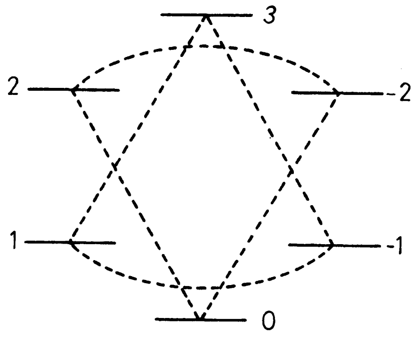

Fig. 4. The coupling of the orbitals in Eqs. 34, 35 by dashed lines.

where

$$\omega_{i,\sigma} = \varepsilon_i + n_{-\sigma} I. \tag{36}$$

The one-electron energies given by the eigenvalues of Eqs. 34 and 35 are expressed as

$$\tilde{\varepsilon}_i^\sigma = \tilde{\omega}_i^\sigma + n_{-\sigma} I, \tag{37}$$

where

$$\begin{aligned}
\tilde{\omega}_1^\sigma &= \frac{1}{2}(-\beta + C_\sigma - \gamma_+^\sigma), \\
\tilde{\omega}_2^\sigma &= -\beta - C_\sigma, \\
\tilde{\omega}_3^\sigma &= \frac{1}{2}(\beta + C_\sigma - \gamma_-^\sigma), \\
\tilde{\omega}_4^\sigma &= \beta - C_\sigma, \\
\tilde{\omega}_5^\sigma &= \frac{1}{2}(-\beta + C_\sigma + \gamma_+^\sigma), \\
\tilde{\omega}_6^\sigma &= \frac{1}{2}(\beta + C_\sigma + \gamma_-^\sigma), \\
\gamma_\pm^\sigma &= 3\sqrt{\beta^2 \pm (2/3)\beta C_\sigma + C_\sigma^2}.
\end{aligned} \tag{38}$$

Then, Green's functions are solved as

$$\begin{aligned}
G_{0,0}^\sigma(\varepsilon) &= \frac{\varepsilon - \tilde{\omega}_2^\sigma - C_\sigma}{Det_2^\sigma(\varepsilon)}, \\
G_{1,1}^\sigma(\varepsilon) &= G_{-1,-1}^\sigma(\varepsilon) = \frac{1}{2}\left\{\frac{\varepsilon - \tilde{\omega}_3^\sigma}{Det_1^\sigma(\varepsilon)} + \frac{1}{\varepsilon - \tilde{\varepsilon}_2^\sigma}\right\}, \\
G_{2,2}^\sigma(\varepsilon) &= G_{-2,-2}^\sigma(\varepsilon) = \frac{1}{2}\left\{\frac{\varepsilon - \tilde{\omega}_0^\sigma}{Det_2^\sigma(\varepsilon)} + \frac{1}{\varepsilon - \tilde{\varepsilon}_4^\sigma}\right\}, \\
G_{3,3}^\sigma(\varepsilon) &= \frac{\varepsilon - \tilde{\omega}_1^\sigma - C_\sigma}{Det_1^\sigma(\varepsilon)},
\end{aligned} \tag{39}$$

and

$$\begin{aligned}
G_{-1,1}^\sigma(\varepsilon) &= G_{1,-1}^\sigma(\varepsilon) = \frac{1}{2}\left\{\frac{\varepsilon - \tilde{\omega}_3^\sigma}{Det_1^\sigma(\varepsilon)} - \frac{1}{\varepsilon - \tilde{\varepsilon}_2^\sigma}\right\}, \\
G_{-2,2}^\sigma(\varepsilon) &= G_{2,-2}^\sigma(\varepsilon) = \frac{1}{2}\left\{\frac{\varepsilon - \tilde{\omega}_0^\sigma}{Det_2^\sigma(\varepsilon)} - \frac{1}{\varepsilon - \tilde{\varepsilon}_4^\sigma}\right\}, \\
G_{3,1}^\sigma(\varepsilon) &= G_{1,3}^\sigma(\varepsilon) = G_{3,-1}^\sigma(\varepsilon) = G_{-1,3}^\sigma(\varepsilon) = \frac{C_\sigma}{Det_1^\sigma(\varepsilon)}, \\
G_{0,2}^\sigma(\varepsilon) &= G_{2,0}^\sigma(\varepsilon) = G_{0,-2}^\sigma(\varepsilon) = G_{-2,0}^\sigma(\varepsilon) = \frac{C_\sigma}{Det_2^\sigma(\varepsilon)},
\end{aligned} \tag{40}$$

TABLE 1. THE SELF-CONSISTENT SOLUTIONS FOR THE WEAK REPULSION

	$\Delta\alpha>0$	$\Delta\alpha<0$
$D+$	$-1/2I$	$1/2I$
$D-$	0	0
$C+$	$1/6(gQ+\Delta\alpha)$	$-1/6(gQ+\lvert\Delta\alpha\rvert)$
$C-$	$-I/12+1/6(gQ+\Delta\alpha)$	$I/12-1/6(gQ+\lvert\Delta\alpha\rvert)$
Δn_r	$1/6(1-\cos 2\pi/3r)$	$1/6(1+\cos 2\pi/3r)$
S_r	$1/12(1-\cos 2\pi/3r)$	$1/12(1+\cos 2\pi/3r)$
φ	0	π

Δn_r is the distribution of the excess charge normalized as $\sum \Delta n_r = 1$. S_r is the spin distribution.

where

$$\begin{aligned}
Det_1^\sigma(\varepsilon) &= (\varepsilon - \tilde{\varepsilon}_3^\sigma)(\varepsilon - \tilde{\varepsilon}_6^\sigma), \\
Det_2^\sigma(\varepsilon) &= (\varepsilon - \tilde{\varepsilon}_5^\sigma)(\varepsilon - \tilde{\varepsilon}_1^\sigma).
\end{aligned} \tag{41}$$

Analytic Solutions in Limiting Cases

The Green's functions, which is dependent on the potential C_σ, must be solved self-consistently with Eqs. 32 and 33. The equations are solved numerically as shown in the next section. Here we give the analytic solutions for two limiting cases of the weak and strong repulsion, as follows.

1. Weak repulsion $\beta \gg |C_\sigma|$ $(I \ll \beta)$

In this case the essential features of the one-electron theory described above are remain unchanged. The occupied levels are in ascending order

$$\begin{aligned}
&\omega_1^+,\ \omega_2^+,\ \omega_3^+,\ \omega_4^+,\ \omega_1^-,\ \omega_2^-,\ \omega_3^- \quad \text{for } \Delta\alpha > 0 \\
&\omega_1^+,\ \omega_3^+,\ \omega_2^+,\ \omega_5^+,\ \omega_1^-,\ \omega_3^-,\ \omega_2^- \quad \text{for } \Delta\alpha < 0.
\end{aligned} \tag{42}$$

The self-consistent solution in the leading order in I/β are listed in Table 1. The real and small parameter of expansion is $|C_\sigma|/\beta$, but not I/β. The former is small as far as I is not too large even if it exceeds β, as will be demonstrated numerically.

The energy gain of the distortion is given by

$$\begin{aligned}
\Delta E &= E - E_0 \\
&= -\frac{1}{6}(gQ + |\Delta\alpha|) + \frac{M}{6}\Omega^2 Q^2,
\end{aligned} \tag{43}$$

where E_0 is the H. F. energy of undistorted configuration of the benzene anion,

$$E_0 = -7\beta + I. \tag{44}$$

The magnitude of Q for the equilibrium configuration is determined by the minimization of Eq. 43 as

$$Q_0 = g/(2M\Omega^2). \tag{45}$$

Equations 43 and 45 agree with the results in the one-electron theory.

2. Strong repulsion $\beta \ll |C_\sigma|$ $(I \gg \beta)$

The occupied levels are the same as Eq. 42. The

Table 2. Two classes of the self-consistent solutions for the strong repulsion, one stable (A) and one unstable (B)

	A (stable)	B (unstable)
$D+$	$-2I$	I
$D-$	$3/2I$	$-3/2I$
$C+$	$I/4+1/6(gQ+\Delta\alpha)$	$-I/4+1/6(gQ+\|\Delta\alpha\|)$
$C-$	$-I/3+1/6(gQ+\Delta\alpha)$	$I/6+1/6(gQ+\|\Delta\alpha\|)$
Δn_r	$1/6(1-\cos 2\pi/3r)$	$1/6(1-\cos 2\pi/3r)$
S_r	$1/12(1-7\cos 2\pi/3r)$	$1/12(1+5\cos 2\pi/3r)$
φ	0	0

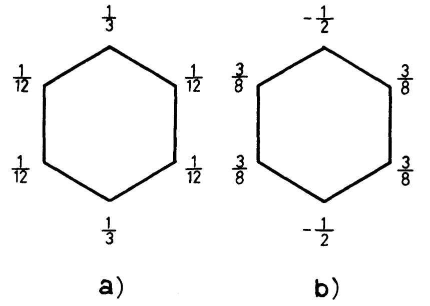

Fig. 5. a) Excess charge distribution, b) Spin distribution.

solutions are given in Table 2. In this case two classes of self-consistent solutions A and B are possible. The energy gain of A and B are, respectively

$$\Delta E_A = I + \beta - \frac{1}{6}(gQ+\Delta\alpha) + \frac{M}{6}\Omega^2 Q^2, \tag{46}$$

$$\Delta E_B = -\frac{1}{2}I + \beta - \frac{1}{6}(gQ+\Delta\alpha) + \frac{M}{6}\Omega^2 Q^2. \tag{47}$$

As long as $I \gg \beta$, the energy of A is lower than that of B irrespective of the sign of $\Delta\alpha$, so that A is the stable configuration. The minimum of Eq. 46 gives Q_0 as the same as Eq. 45. The distributions of the excess charge and spin are illustrated in Fig. 5. The effect of the electron-repulsion is drastic. The odd electron polarizes the electrons at the levels of $n=0$, ± 1 which already exist in the neutral benzene, and leads to the negative spin density at sites 3 and 6.

Numerical Results

For the whole range of I, the numerical analysis is performed. We give values of the parameters as follows.

$$\Delta\alpha = 0.01,$$
$$g = 0.04,$$
$$Q = 0.02.$$

The sign of $\Delta\alpha$ represents the electrophilicity or the nucleophilicity of the solvent. The absolute value of $\Delta\alpha$ and g can be selected rather arbitrarily, because they affect hardly on the results. Q is the value that lets the total energy minimize on $I=3$ (this value of I would probably correspond to the electron correlation for the benzene molecule.).

The results are shown in Figs. 6—10. All the resultant values for $I \geqq 15$ are very close to the analytic solutions given in the previous section. The I dependence of C_σ, D_σ/I and that of energy E are represented in Figs. 6 and 7, respectively. As illustrated in figures, two classes of self-consistent solutions, one stable and one unstable, exist as mentioned before. The solid and dashed curves correspond to the stable solution A and the unstable one B, respectively. The orbital patterns corresponding to the two classes of solutions for $I=3$ and 12 are illustrsted in Fig. 8. It is easy to see that the patterns for unstable solution does not give the proper ground state.

Figure 9 shows the behavior of the charge density and the spin density *versus I*. In this figure the solid and dashed curves correspond to the values on sites 1 and 6, respectively.

Figure 10 represents the relation between the total energy E and the displacement Q, and shows the stabilization of energy due to the Jahn-Teller effect. On calculating the total energy, we assigned the value of 4.12 for the parameter $M\Omega^2$ which is calculated from

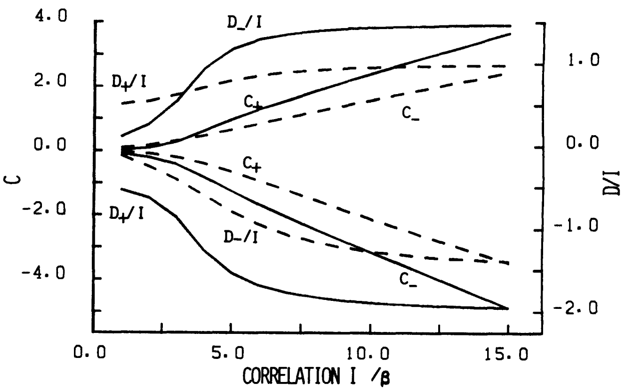

Fig. 6. C_σ and D_σ/I vs. I. I is represented in the unit $\beta=1$. We give values of the parameters as follows: $\Delta\alpha=0.01$, $g=0.04$, $Q=0.02$. The solid and dashed curves correspond to the stable and unstable solutions, respectively.

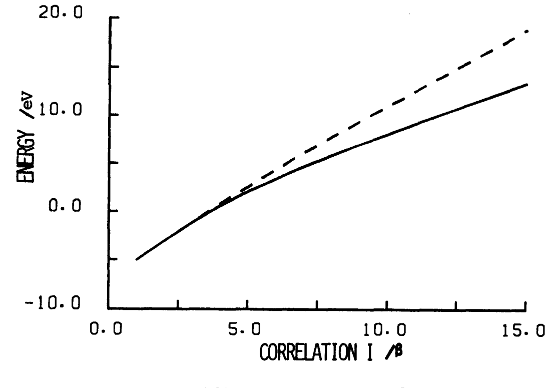

Fig. 7. E vs. I. All parameters and curves are the same as Fig. 6.

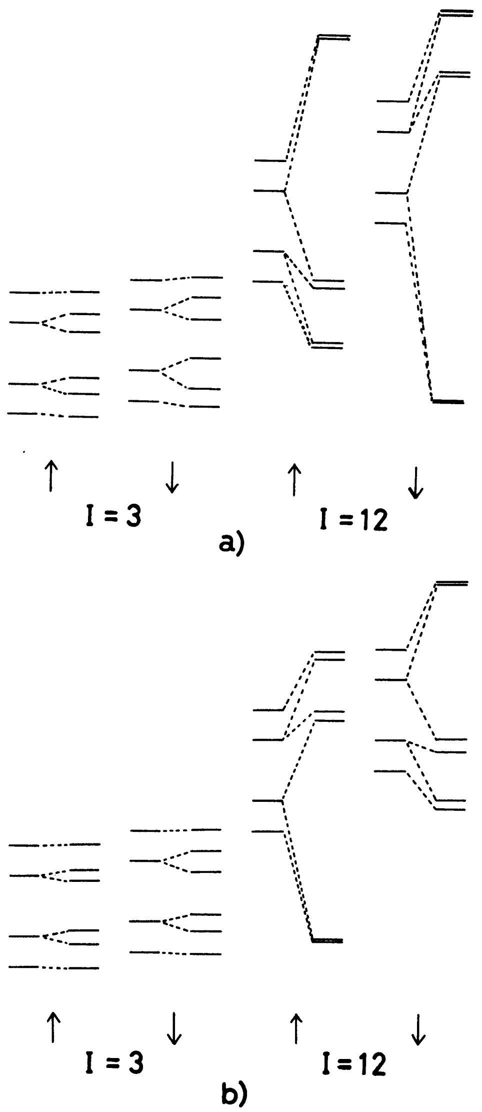

Fig. 8. The orbital patterns for the undistorted and distorted cases with $I=3$ and 12 are compared. a) Orbital patterns for stable solution, b) For unstable one. The up and down arrows represent the up and down spin orbitals, respectively. All parameters are the same as Fig. 6.

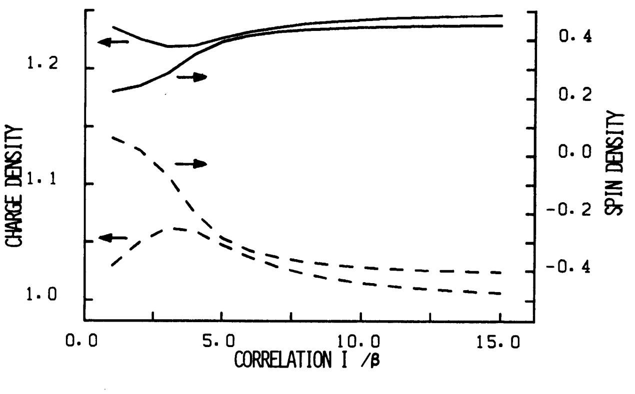

Fig. 9. The charge density and the spin density *vs.* I. The solid and dashed curves correspond to the densities for the case of the stable solution on sites 1 and 6, respectively. All parameters are the same as Fig. 6.

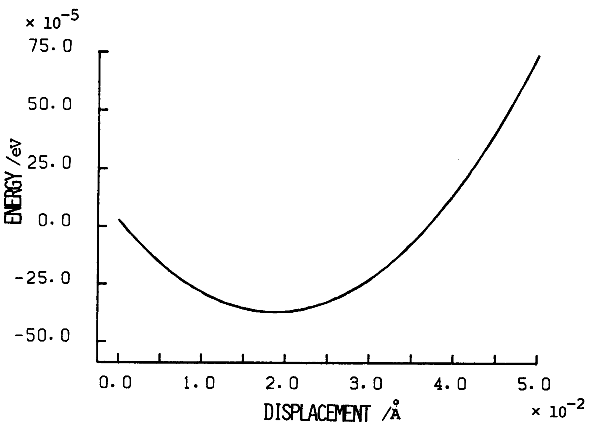

Fig. 10. The energy gain due to the distortion Q. The energy is expressed in eV and Q in Å. $\Delta\alpha=0.01$, $g=0.04$, $I=3$, $M\Omega^2=4.12$.

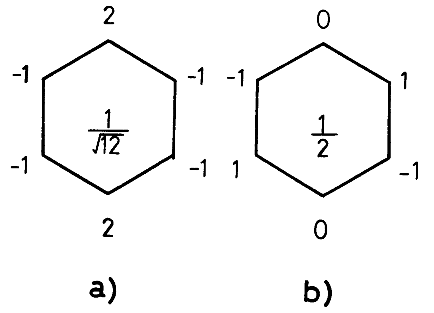

Fig. 11. The wave functions of unoccupied and degenerate levels of benzene. The numbers inside the rings are normalization factor.

the force constant of the E_g^+ vibronic mode of the benzene molecule.[13] The energy is minimized at Q=0.02 Å.

Concluding Remarks

We have analyzed the Jahn-Teller distortion of the benzene anion on the basis of the modified P.P.P. models. As far as the repulsion is weak, our results confirm the simple theory considering only the odd electron of the anion.[3] But if the repulsion becomes strong, *i.e.*, $I/\beta > 15$ the effect of other π electrons becomes significant. This effect appears more remarkably on the distribution of the spin than that of the charge. The discrepancy between the distributions of the spin and charge originates from the exchange interaction between the π electrons which is not considered in the single electron theory.

We wish to stress a few points. Look at Fig. 11 which displays the amplitude of the unoccupied, degenerate wave functions with $n=\pm 2$ of benzene. The odd electron of the benzene anion is equally distributed on these two states. However, this picture is only for pictorial understanding and each pattern of the charge density distribution given by a) or b) in Fig. 11 is of less meaning by itself, but the mean of them would correspond to usual experimental observations. This aspect holds even if the vibronic interaction is introduced in Eq. 7 to remove the degeneracy, since the phase of the electron distribution remains still arbitrary.

The external perturbation which reduces the molecular symmetry from C_6 to C_2 and fixes the phase φ is given by the last term of Eq. 7. Let this perturbation work during a characteristic time τ. So long as τ is large enough compared with the time scale during which the position determining experimental observation can be made, the states indicated in Fig. 11 a) and b), and the similar ones in Fig. 5 become meaningfull. The curious distributions of the odd electron density or the spin density shown in Fig. 5 are to be understood as an event taking place in the characteristic time τ. In other words, we may imagine that during this time the solvent molecules are located near the positions 3 and 6. If τ is quite small, we would observe time averaged uniform distributions for the charge and spin densities. Such consideration plays an important role in the analysis of the observed ESR spectra of this ion.[14)]

Finally we stress that the negative spin densities at sites 3 and 6 induced by the strong electron interaction are interesting, because it makes an excellent contrast to the case of the single electron theories.

Appendix

In this appendix we derive Eq. 27 for the total energy.[15)] First, the Hamiltonian (Eqs. 5—7) are re-written as

$$H_{el} = H_1 + H_2, \tag{48}$$

where

$$\begin{aligned} H_1 = &-\beta\sum_{r,\sigma}(a^+_{r\sigma}a_{r+1\sigma}+\text{h.c.}) \\ &+\frac{1}{2}\Delta\alpha\sum_{r,\sigma}n_{r\sigma}(\delta_{r,3}+\delta_{r,6}) + g\sum_{r,\sigma}Q_r n_{r\sigma}, \end{aligned} \tag{49}$$

$$H_2 = \frac{1}{2}I\sum_{r,\sigma}n_{r\sigma}n_{r-\sigma}. \tag{50}$$

The expectation value of H_1 is expressed as

$$\begin{aligned} \langle H_1\rangle = &-i[-\beta\sum_{r,\sigma}\{G^{\sigma}_{r+1,r}(t)+G^{\sigma}_{r-1,r}(t)\} \\ &+\sum_{r,\sigma}(gQ_r+\frac{1}{2}\Delta\alpha(\delta_{r,3}+\delta_{r,6})G^{\sigma}_{r,r}(t)]_{t\to 0^-}. \end{aligned} \tag{51}$$

The expectation value of H_2 is written as

$$\langle H_2\rangle = \frac{1}{2}I\sum_{r,\sigma}\langle a^+_{r\sigma}a^+_{r-\sigma}a_{r-\sigma}a_{r\sigma}\rangle. \tag{52}$$

Comparing Eq. 52 with Eqs. 28 and 29, we obtain

$$\begin{aligned} \langle H_2\rangle = &-\frac{i}{2}\sum_{r,\sigma}[(i\frac{\partial}{\partial t}-gQ_r-\Delta\alpha\delta_{r,6})G^{\sigma}_{r,r}(t) \\ &+\beta\{G^{\sigma}_{r+1,r}(t)+G^{\sigma}_{r-1,r}(t)\}]_{t\to 0^-}. \end{aligned} \tag{53}$$

Adding Eqs. 51, 53, and the elastic energy Eq. 8, we obtain Eq. 27.

References

1) A. D. Liehr, *Z. Phys. Chem.*, **9**, 338 (1956).

2) L. C. Snyder, *J. Chem. Phys.*, **33**, 619 (1960).

3) W. D. Hobey and A. D. McLachlan, *J. Chem. Phys.*, **33**, 1695 (1960).

4) H. M. McConnel and A. D. McLachlan, *J. Chem. Phys.*, **34**, 1 (1961).

5) M. Kimura, K. Nishikawa, and S. Aono, *Bull. Chem. Soc. Jpn.*, **54**, 3619 (1981).

6) K. Nishikawa, M. Kimura, and S. Aono, *Bull. Chem. Soc. Jpn.*, **54**, 3624 (1981).

7) W. P. Su, J. R. Schriefer, and A. J. Heeger, *Phys. Rev.*, **B34**, 2099 (1980).

8) T. Holstein, *Ann. Phys.*, **8**, 325 (1959).

9) S. Kivelson and D. E. Heim, *Phys. Rev.*, **B26**, 4278 (1982).

10) Y. Toyozawa, *J. Phys. Soc. Jpn.*, **50**, 1861 (1981).

11) K. Nasu and Y. Toyozawa, *J. Phys. Soc. Jpn.*, **51**, 2098 (1982).

12) J. Hubbard, *Proc. Roy. Soc.;* **A276**, 238 (1963).

13) S. Mizushima and T. Shimanouchi, "Infrared Absorption and Raman Effect," Kyoritsu publishing, Tokyo, (1985).

14) M. G. Townsent and S. I. Weissman, *J. Chem. Phys.*, **32**, 309 (1960).

15) A. L. Fetter and J. D. Walecka, "Quantum Theory of Many-Particle Systems," McGraw-Hill, New York, (1971).